



HAL
open science

Corrective GUSB transfer to the canine mucopolysaccharidosis VII cornea using a helper-dependent canine adenovirus vector.

Nicolas Serratrice, Aurelie Cubizolle, Sandy Ibanes, Nadine Mestre-Francés, Neus Bayo-Puxan, Sophie Creyssels, Aurelie Gennetier, Florence Bernex, Jean-Michel Verdier, Mark E Haskins, et al.

► **To cite this version:**

Nicolas Serratrice, Aurelie Cubizolle, Sandy Ibanes, Nadine Mestre-Francés, Neus Bayo-Puxan, et al.. Corrective GUSB transfer to the canine mucopolysaccharidosis VII cornea using a helper-dependent canine adenovirus vector.. *Journal of Controlled Release*, 2014, 181, pp.22-31. 10.1016/j.jconrel.2014.02.022 . hal-01104769

HAL Id: hal-01104769

<https://hal.science/hal-01104769>

Submitted on 8 Feb 2019

HAL is a multi-disciplinary open access archive for the deposit and dissemination of scientific research documents, whether they are published or not. The documents may come from teaching and research institutions in France or abroad, or from public or private research centers.

L'archive ouverte pluridisciplinaire **HAL**, est destinée au dépôt et à la diffusion de documents scientifiques de niveau recherche, publiés ou non, émanant des établissements d'enseignement et de recherche français ou étrangers, des laboratoires publics ou privés.



Published in final edited form as:

J Control Release. 2014 May 10; 181: 22–31. doi:10.1016/j.jconrel.2014.02.022.

Corrective GUSB transfer to the canine mucopolysaccharidosis VII cornea using a helper-dependent canine adenovirus vector

Nicolas Serratrice^{a,b,c,1}, Aurelie Cubizolle^{a,b,c,1}, Sandy Ibanes^{a,b,c}, Nadine Mestre-Francés^{c,d,e}, Neus Bayo-Puxan^{a,b,c}, Sophie Creyssels^{a,b,c}, Aurelie Gennetier^{a,b,c}, Florence Bernex^f, Jean-Michel Verdier^{c,d,e}, Mark E. Haskins^g, Guilhem Couderc^h, Francois Malecaze^{i,j}, Vasiliki Kalatzis^{a,b,c}, and Eric J. Kremer^{a,b,c,*}

^aInstitut de Génétique Moléculaire de Montpellier, CNRS 5535, Montpellier, France

^bUniversité de Montpellier I, Montpellier, France

^cUniversité Montpellier 2, Montpellier, France

^dInserm U710, Montpellier, France

^eEcole Pratique des Hautes Etudes, Paris, France

^fInstitut Régional du Cancer Montpellier, Inserm U896, Montpellier, France

^gDepartment of Pathobiology, School of Veterinary Medicine, School of Veterinary Medicine, University of Pennsylvania, Philadelphia, PA, USA

^hTissue Bank, Centre Hospitalier Régional Universitaire de Montpellier, Montpellier, France

ⁱInserm U563, Toulouse, France

^jDépartement d'Ophtalmologie, Hôpital Purpan, Toulouse, France

Abstract

Corneal transparency is maintained, in part, by specialized fibroblasts called keratocytes, which reside in the fibrous lamellae of the stroma. Corneal clouding, a condition that impairs visual acuity, is associated with numerous diseases, including mucopolysaccharidosis (MPS) type VII. MPS VII is due to deficiency in β -glucuronidase (β -glu) enzymatic activity, which leads to accumulation of glycosaminoglycans (GAGs), and secondary accumulation of gangliosides. Here, we tested the efficacy of canine adenovirus type 2 (CAV-2) vectors to transduce keratocyte *in vivo* in mice and nonhuman primates, and *ex vivo* in dog and human corneal explants. Following efficacy studies, we asked if we could treat corneal clouding by the injection a helper-dependent (HD) CAV-2 vector (HD-RIGIE) harboring the human cDNA coding for β -glu (GUSB) in the canine MPS VII cornea. β -Glu activity, GAG content, and lysosome morphology and physiopathology were analyzed. We found that HD-RIGIE injections efficiently transduced coxsackievirus adenovirus receptor-expressing keratocytes in the four species and, compared to mock-injected controls, improved the pathology in the canine MPS VII cornea. The key criterion

*Corresponding author at: IGMM, CNRS 5535, 1919 Route de Mende, 34293 Montpellier, France. Tel.: +33 4 34 35 96 72; fax: +33 4 34 35 96 34. eric.kremer@igmm.cnrs.fr (E.J. Kremer).

¹Equal contribution.

Supplementary data to this article can be found online at <http://dx.doi.org/10.1016/j.jconrel.2014.02.022>.

to corrective therapy was the steady controlled release of β -glu and its diffusion throughout the collagen-dense stroma. These data support the continued evaluation of HD CAV-2 vectors to treat diseases affecting corneal keratocytes.

Keywords

Tissue engineering; Cornea; Keratocytes; Mucopolysaccharidosis; Lysosomal storage disorders; β -Glucuronidase; Clouding; Primates

1. Introduction

The cornea is the transparent avascular tissue at the most anterior surface of the primate eye. It is mainly composed of an external stratified epithelium, an endothelium made up of a cuboidal monolayer of epithelial-like cells, and a thick collagenous stroma separating the two. The stroma is primarily composed of extracellular matrix that makes up 90% of its thickness. The predominant stromal cell type is the keratocyte, a specialized fibroblast that plays a role in general repair and maintenance. In a number of diseases, including lysosomal storage diseases (LSDs) [1], corneal clouding perturbs visual acuity [2]. Among the approximately 60 LSDs, 11 mucopolysaccharidoses (MPSs) are caused by accumulation of glycosaminoglycans (GAGs) due to deficient lysosomal enzyme activity [3]. Among MPS diseases, MPS VII is an autosomal recessive disorder caused by deficiency in the enzymatic activity of β -glucuronidase (β -glu), a 300-kDa tetrameric hydrolase found in all mammalian cells, except red blood cells. Impaired β -glu activity results in partial degradation of the GAGs chondroitin sulfate, dermatan sulfate, heparan sulfate, and secondary accumulation of gangliosides (GM2 and GM3). Enlarged storage vesicles (lysosomes) are associated with corneal, hepatic, cardiovascular, respiratory, skeletal, and CNS lesions.

Current therapies for some MPS diseases include bone marrow transplantation and enzyme replacement therapy (ERT). The efficacy of these approaches relies on the uptake of secreted enzyme via mannose-6-phosphate receptor for delivery to lysosomes, a pathway dubbed cross correction [4]. Likely because the cornea is avascular, ERT does not prevent corneal clouding. Corneal transplantation has also been tried in MPS VII, but has not stopped recurring disease [2]. Gene transfer offers substantial potential to understand, prevent and treat diseases, yet this strategy also has unique clinical obstacles — in particular the need to assess vector efficacy and safety in healthy and diseased animals. Each viral vector has advantages and drawbacks such as cloning capacity, memory or induced immunity, toxicity, specificity, safety, titer, or efficacy [5]. Gene transfer for LSD-associated corneal clouding has been tested in mice [6] using adenoviruses (Ad), but has not been directly tested in the ~50-fold larger canine or human MPS VII cornea. We previously showed that when canine adenovirus type 2 (CAV-2) vector transduced post-mitotic neurons they could express a transgene for at least 1 year *in vivo* [7,8]. Combining these characteristics with a 30-kb cloning capacity [8], the paucity of cross-reacting human humoral and cellular immunity [9,10], and the inability to induce dendritic cell maturation [11], makes helper-dependent (HD) CAV-2 vectors powerful tools for clinical gene transfer to post-mitotic cells.

In this study, we compared transduction efficacy of CAV-2 and human Ad type 5 (HAd5) vectors *in vivo* in healthy mouse and nonhuman primate corneas, and *ex vivo* in healthy human and canine corneal explants by intrastromal injection. We then tested the potential of HD CAV-2 vectors for corneal therapy in MPS VII dog cornea. We found that CAV-2 vectors efficiently transduced keratocytes throughout the stroma via a single injection. Moreover, a helper-dependent (HD) CAV-2 vector harboring a human β -glu expression cassette (HD-RIGIE) corrected the pathology of the canine MPS VII cornea explants. Yet, this correction will be dependent on β -glu diffusion in the thick collagenous stroma. These encouraging data support the continued evaluation of HD CAV-2 vectors to treat corneal disease associated with MPS VII and possibly other LSDs.

2. Materials & methods

2.1. Cornea collection and organ culture

Human cornea explants were provided by the CHU of Montpellier Tissue Bank as part as the CHU de Montpellier Biobank, and used as conformed to French legislation. Explants were from deceased donors and not usable for grafts due to endothelial density. Cornea explants were also from healthy and MPS VII dogs [12]. *In vivo* injections were in ~2-month old C57BL/6 mice (Charles River Laboratories), and ~6-month old gray mouse lemurs (GML, or *Microcebus murinus*), a nonhuman primate that can be readily bred in captivity. Human explants, healthy dogs, mice and GML did not have ocular disease, wounds or infections. Canine MPS VII cornea had mild clouding. Animal care and experiments conformed to European Council Directive 2010/63/EU, and French legislation. The protocols were approved by the Languedoc–Roussillon ethics committee (CEEA-LR1013). Mice, GML and dogs' corneas were cultured in DMEM supplemented with 5% FBS and antibiotics at 32 °C. Human explants were cultured in CorneaMax (EuroBio) at 31 \pm 1 °C.

2.2. Recombinant adenovirus vectors

CAVGFP and AdRFP vectors derived from CAV-2 and HAd5, have been previously described [5,13]. CAVGFP contains aCMV-driven GFP expression cassette and AdRFP contains a CMV-driven DSRed II expression cassette. Minimum titers were 1×10^{12} physical particles (pp)/ml. Two helper-dependent (HD) CAV-2 (HD CAV-2) vector expressing GFP (HD-GFP) [8] and β -glucuronidase and GFP (HD-RIGIE) [14,15] were used. HD-RIGIE production and quality controls were performed as described [8]. The titers for HD-GFP and HD-RIGIE were 3×10^{11} pp/ml and 1.3×10^{12} pp/ml, respectively.

2.2.1. Production of HcivD-RIGIE and HD-GFP vectors—HD-RIGIE expressed the human GUSB cDNA and GFP under the control of a Rous sarcoma virus promoter. The RIGIE cassette (RSV-IVS-GUSB-IRES-EGFP) was constructed using classic molecular biology techniques. The human GUSB cDNA was a gift from William Sly, University of St. Louis. AscI/NotI-digested pHD-RIGIE or pHD-GFP was transfected into 5×10^6 DKZeo cells using 18 μ l of Turbofect (Fermentas) for 10 μ g of linearized DNA/10 cm plate. The cells were infected with 100 pp of helper vector/cell. GFP + cells were collected by flow cytometry 24 h post-transfection, re-plated, and lysed by three freeze/thaw cycles 20 h later.

Cells were sorted after transfection until 2×10^6 of GFP + cells were isolated. The cleared lysates were then incubated on a fresh monolayer of DKZeo cells using helper vector JB 5. Twenty-four hours postinfection, GFP + cells were sorted by flow cytometry, re-plated, and lysed by three freeze/thaw cycles 20 h later. The cleared lysate was used for amplification until 3×10^7 GFP + cells were obtained. At each amplification step, DKZeo cells were co-infected with 100 pp/cell of helper vector. The last amplification was performed using $\sim 8 \times 10^8$ DKCre cells without adding helper vector. JB 5 contains a loxP-flanked packaging domains and a RSV-lacZ expression cassette [8,16]. When propagated in DKCre cells, a ~ 900 bp fragment containing the packaging domain and part of the RSV promoter was excised (floxed), and the resulting 32.3 kb vector was rendered packaging-deficient [8]. The helper vector retained a minimal part of the RSV promoter, which promoted lacZ expression. To test the level of helper contamination in helper-dependent vector preparations, β -galactosidase activity was assayed by X-gal staining. HD-RIGIE and HD-GFP were purified by triple banding on CsCl density gradients: an initial step gradient of 1.25 g/ml and 1.45 g/ml, and then two self-forming isopycnic gradients using 1.32 g/ml CsCl as previously described [8]. The purified stock was stored at -80°C in PBS/10% glycerol.

2.3. Intrastromal injections

2.3.1. Mouse and GML corneas—General anesthesia was induced with xylazine/ketamine mix (0.01 ml/kg, intraperitoneal) for mice and with Imalgene 500 (0.01 ml/kg, intraperitoneal) for GML. Local anesthesia using 1% tetracaine (Faure, collyre) was used before injections. In each animal, one eye was injected, and the other used as control. When needed, corneas were also humidified with a sponge during the procedure. Injections were performed using a surgical microscope with a 33-gauge needle (Hamilton Co) attached to a 10- μl syringe. A small tunnel was created using a microsurgery blade across the epithelium at the pericentral zone (beginning of the thickest part of the cornea) in mice and at the limbus in GML. This tunnel was used to tangentially introduce the needle into the stroma. The volume injected was 20 μl in mouse, 30 μl in GML and 200 μl in human and dog corneas. 1×10^9 pp of vector was injected into the stroma of mice and GML. 5×10^9 pp of each vector was injected in dog and human corneal explants. Vector dilutions were in PBS. For the *in vivo* injections, no animals died prematurely and edema spontaneously reversed.

2.4. Imagery

For *in vivo* imaging, the animals were maintained under isoflurane/oxygen mask during corneal examination. A modified M2BIO stereomicroscope combining a stereo-zoom with long distance macro-objectives (1 to 2.5 \times) and a mono-objective (20 \times) permitted a magnification of 15 to 1200 \times with a large working distance (1.2 to 2 cm). The microscope contained an epifluorescence system (GFP filters), and an X/Y/Z motorized platform, and acquisition performed with a CCD (charged-coupled device) camera (Hamamatsu).

2.5. Cornea preparation for confocal microscopy and histology

Corneal explants were fixed in 4% paraformaldehyde overnight, transferred to 30% sucrose/PBS solution overnight and embedded in OCT compound (Tissue-Tek, Sakura).

Ten-micron-thick transversal frozen sections were cut with a cryo-microtome. Sections were stained with 1 µg/ml bis-benzimide Hoechst (Sigma-Aldrich) and mounted with Vectashield (DAKO). For the immunofluorescence CD34 staining, sections were thawed for 15 min at room temperature, washed in PBS for 15 min to remove OCT, permeabilized (0.1% Triton) for 15 min at room temperature and blocked in 2.5% horse serum/0.5% BSA/0.1% Triton for 30 min. Primary antibodies were incubated on sections overnight at 4 °C, and the secondary antibody incubated 90 min, at room temperature prior to Hoechst labeling and mounting. For the human corneas, the primary antibody used was 1:100 mouse anti-human CD34 (clone B1-3C5; AbCam, Cambridge, UK) and the secondary antibody 1:500 goat anti-mouse IgG-Alexa546 (Molecular probes, Invitrogen). For the dog corneas, the primary antibody used was 1:100 mouse anti-dog CD34-PE (clone 1H6, eBioscience) and the secondary antibody 1:500 goat anti-mouse IgG-Alexa Fluor 546 (Molecular probes, Invitrogen). Observations and acquisitions were performed with either a Zeiss LSM510 or a LEICA SP5 laser scanning confocal microscope. Image analyses were performed using MetaMorph software.

2.6. Transmission electron microscopy (TEM)

Corneas were immersed in a solution of 2.5% glutaraldehyde in Sorensen's buffer (0.1 M, pH 7.4) overnight at 4 °C, rinsed in Sorensen's buffer, and post-fixed in a 0.5% osmic acid for 2 h at room temperature. After two rinses in Sorensen's buffer, the corneas were dehydrated in a graded series of ethanol solutions (30–100%). The corneas were embedded in EmBed 812 using an automated microwave tissue processor for EM, Leica EM AMW. Thin sections (70 nm; Leica–Reichert Ultracut E) were collected at different levels of each block. These sections were counterstained with uranyl acetate and observed using a Hitachi 7100 transmission electron microscope.

2.7. Quantitative and histological analysis of β-glu activity

β-Glu activity in whole corneas was determined using a fluorometric assay as described previously [17]. Briefly, corneas were homogenized in RIPA buffer (20 mM Tris pH 7.5, 150 mM NaCl, 1% NP40, 0.5% sodium deoxycholate, 0.1% SDS) and centrifuged at 11,600 g for 5 min to remove debris. β-Glu activity was measured using 4-methyl-umberyferryl β-D-glucuronide (SIGMA) as substrate. β-Glu activity is expressed in nmol of 4-methyl-umberyferryl β-D-glucuronide liberated/h/mg total proteins. Histochemical detection of β-glu was performed on 10- or 16-µm-thick frozen sections using naphthol-AS-BI-β-D-glucuronide (SIGMA) as substrate overnight. Sections were then mounted in a nonaqueous medium (MOUNTEX medium). Observations and acquisitions were performed with a NanoZoomer (Hamamatsu, Japan).

2.7.1. Histological analysis of GAG storage—Sections were thawed for 15 min at room temperature, washed in distilled H₂O for 10 min and immersed in toluidine blue (0.5% toluidine blue + 1% Borax) for 30 min at room temperature. Sections were washed in distilled H₂O for 30 s and dehydrated in 95% ethanol for 3 min, in 100% ethanol for 3 min and in xylene for 5 min. Sections were dried at room temperature and mounted in a nonaqueous medium (MOUNTEX medium). Observations and acquisitions were performed with a NanoZoomer.

3. Results

3.1. CAV-2 vectors efficiently transduced mouse, gray mouse lemur, and human corneal keratocytes

Translational medicine, including gene transfer, has often been tested in laboratory rodents prior to studies in more challenging animals or progression to clinical use. Mice have historically been used as preclinical models for gene transfer and may faithfully mimic vector tropism in humans. However, the conclusions garnered from many studies have shown that the clinical relevance can be problematic. Therefore, we compared the efficacy of CAV-2 vector transduction of keratocytes in the cornea of four species, including humans. We previously showed that CAV-2 and HAd5 vector efficacy in murine cornea was feasible (see supplementary data in [18]). To compare under optimal conditions, we co-injected CAVGFP [13], a CAV-2 vector expressing GFP, and AdRFP [5], a HAd5 vector expressing DsRed II in the mouse stroma. Forty-eight hours postinjection, *in vivo* imaging using stereomicroscopy permitted real time evaluation of GFP expression (Fig. 1A). GFP expression was detected in all mice and generally throughout the corneas. Corneas were then removed, fixed, embedded, sectioned and analyzed by confocal microscopy. Consistent with the *in vivo* images, sagittal sections of mouse corneas showed GFP⁺ cells throughout the stroma (Fig. 1B). The efficacy of the CAV-2 and HAd5 vectors was comparable: the number of cells expressing GFP and DsRed was similar in most areas. GFP⁺, DsRed⁺, and GFP⁺/DsRed⁺ cells (Fig. 1C–E) were detected, consistent with an overlapping tropism between the vectors.

CAV-2 and HAd5 vector efficacy was compared *in vivo* in the corneas of gray mouse lemurs (GML) by co-injecting CAVGFP and AdRFP. As with the mouse injections, a transient edema of the cornea occurred, but the integrity and transparency of the structure returned to normal the following day. As with the mice, real-time *in vivo* imaging suggested widespread GFP expression throughout the stroma in the GML (Fig. 1F). As above, corneas were removed and analyzed by confocal microscopy. Consistent with the *in vivo* images, sagittal sections of GML corneas showed GFP⁺ cells throughout the stroma (Fig. 1G). CAV-2 and HAd5 vector efficacy was similar in most areas. GFP⁺, DsRed⁺, and GFP⁺/DsRed⁺ (Fig. 1H–J) cells were detected.

Intrastromal injections of CAVGFP and AdRFP in human explants led to transduced cells from the central to the limbal zone of the cornea (Fig. 1K & L). In contrast to the *in vivo* results with mice and GML, very few DsRed⁺ cells were detected at this dose (5×10^9 pp, n = 3), while CAVGFP was efficient (Fig. 1M–O). The cell morphology, the location, and the abundance suggested CAV-2 vectors were transducing keratocytes. To address this using a histological approach, we stained for CD34 expression, a marker of keratocytes in some species [19]. We found that CAV-2 vector preferentially transduced CD34⁺ cells and, therefore, keratocytes (Fig. 1P–R). As we previously proposed [20] that CAV-2 vector transduction was dependent on the expression of the coxsackievirus and adenovirus receptor (CAR) [21–23], we asked if CD34⁺ keratocytes also expressed CAR. Sagittal sections of human cornea were stained with anti-CAR and anti-CD34 antibodies. Consistent with CAV-2 vector transduction, CD34⁺ cells were also CAR⁺ (Fig. 1S–U).

3.2. HD-RIGIE preferentially transduced keratocytes in healthy & MPS VII dog cornea

Corneal clouding is associated with most mucopolysaccharidoses [24], including MPS VII. Studies using the murine MPS VII cornea have suggested that gene transfer could reverse some of the histological anomalies, in particular GAG storage [6]. However, large, long-lived animals with similar diseases may be more predictive of clinical efficacy. CAV-2 and HAd5 vector efficacy was compared in the canine cornea, which also has a size more closely resembling that of the human cornea. Whole explant imaging suggested that CAV-2 vector efficiently transduced cells throughout the canine cornea (Fig. 2A). Analyses of sagittal sections of the injected canine corneas were also consistent with efficient CAV-2-mediated gene transfer (Fig. 2B). Consistent with previous results in the mouse and GML corneas, CAV-2 efficacy (GFP⁺ cells) was similar to that of HAd5 (DsRed⁺ cells) (Fig. 2C–E).

We then asked if a CAV-2 vector could efficiently transduce and correct diseased cornea. To address this we created HD-RIGIE, an HD CAV-2 vector harboring the cDNA of human GUSB (hGUSB), an IRES and GFP (Fig. 2F). HD-RIGIE allowed the identification of transduced cells via GFP expression and the biodistribution of β -glu enzymatic activity. In contrast to GFP, β -glu can be released from cells and internalized by neighboring cells via the mannose 6-phosphate receptor. When HD-RIGIE was injected into healthy (Fig. 2G–I) and MPS VII canine corneas (Fig. 2J–L), transduction of CD34⁺ cells was efficient.

The ability of HD-RIGIE to generate β -glu activity in healthy and MPS VII canine cornea was then tested. Initially, β -glu activity was quantified biochemically using cell lysates (Table 1). In healthy and MPS VII HD-RIGIE-injected corneas, β -glu activity was >10-fold higher compared to noninjected. β -Glu activity can also be detected using a less sensitive *in situ* colorimetric staining (Fig. 3A–D). Of note, β -glu activity is undetectable even in healthy canine cornea using this approach. However, in vector-injected healthy and MPS VII cornea, β -glu activity was detected throughout most of the stroma (Fig. 3B & D). Notably, in most sections there was a gradient in the colorimetric β -glu staining. This could have been due to low vector diffusion in the thick, collagenous extracellular matrix that makes up 90% of the corneal thickness. This gradient would not have been as obvious in the thinner murine MPS VII cornea [18], and therefore accentuate the relevance of the larger diseased cornea. Together, these data are consistent with increased β -glu activity following HD-RIGIE injections.

3.3. HD-RIGIE injection reverses GAG accumulation in MPS VII keratocytes

The histological hallmark of MPS VII disease is large non-staining vacuoles that likely contain GAGs. In healthy corneal stroma and epithelium, cells stained with toluidine blue appear solid blue with no prominent intracellular organelles (Fig. 4A–D). In mock- or HD-GFP-injected corneas from MPS VII dogs, non-staining vesicles can be readily detected in the cytoplasm of keratocytes and epithelial cells (Fig. 4E–H). In addition to non-staining vesicles, MPS VII keratocytes were rounder (Fig. 4E & F). At 5 days post-injection of HD-RIGIE in canine MPS VII corneas, the morphology and toluidine blue staining started to resemble keratocytes in healthy dogs (Fig. 4I & K). At 17 days post-injection (Fig. 4J & L),

stroma and epithelial cells presented with further improved morphology and reduced vesicles.

A masked histopathologist then graded the histological anomalies in mock-, HD-GFP-, or HD-RIGIE-injected, healthy and MPS VII corneas (Table 2, and in Fig. 4). Globally, mock-, HD-GFP- and HD-RIGIE-injected healthy canine corneas were scored as “0”, while mock- and HD-GFP-injected MPS VII corneas scored “2–3”. The less severe MPS VII pathology in some corneas was due to the relatively young age of some of the dogs when the corneas were collected (4–6 weeks). Nonetheless, HD-RIGIE-injected MPS VII corneas showed a marked improvement in non-staining vesicles and were globally scored “1–2”. It is likely that keratocytes that were directly transduced by HD-RIGIE were rapidly corrected because of the amount of β -glu activity/cell. Cells that were not HD-RIGIE-transduced, but took up β -glu secreted from the transduced cells, likely were delayed in reducing the size and number of enlarged vesicles because it took longer for the enzyme to reach the cells.

Several MPS disorders, including MPS VII, may induce upregulation of lysosomal and autophagy-related genes via transcription factor EB (TFEB) master regulation [25] in some species. To complement the results showing reduced GAG storage in HD-RIGIE-injected corneas, we also assayed for LAMP1 expression, a marker of lysosomes (Fig. 5). Although LAMP1 may be overexpressed in the MPS VII cells via TFEB, the most prominent phenotype is larger LAMP1⁺ vesicles in MPS VII cells. In healthy keratocytes, LAMP1 expression was faint and in small puncta (Fig. 5A). Throughout the HD-GFP-injected MPS VII cornea, LAMP1 expression was notably more intense and associated with larger structures (Fig. 5B). At 5 days post-HD-RIGIE injections, no notable difference between mock-injected corneas was evident. However, in many areas of “17 day HD-RIGIE-injected corneas”, LAMP1 staining more closely resembled the strength and pattern present in healthy corneas (Fig. 5C–D). To provide quantitative data, we measured the integrated intensity of LAMP1 staining/cell (Fig. 5E). We found a significant difference in intensity between healthy, MPS and HD-RIGIE-injected corneas. Combined, these data supported our conclusion that HD-RIGIE corrected the histological hallmarks of MPS VII in dog corneas.

Distended vesicles in MPS diseases are also readily detected by transmission electron microscopy. Therefore corneas were prepared for ultrastructural analyses. In MPS VII keratocytes, large clear vacuoles are readily apparent (Fig. 6A & B) compared to healthy keratocytes (Fig. 6C & D). At 5 and 17 days post-injection of HD-RIGIE in MPS VII cornea, a notable reduction of the size associated with a decrease in the number of clear staining vacuoles was apparent (Fig. 6E & F). Together, these data are consistent with toluidine blue and LAMP1 staining that suggested improvement of MPS VII-associated histological anomalies in keratocytes.

4. Discussion

The cornea is an ideal target for gene therapy as it is accessible, relatively immune privileged, and easily monitored due to its transparency [26]. Potential applications are the correction of corneal neovascularisation [27,28], scarring [29,30], and the treatment of certain genetic diseases [31]. Corneal anomalies in LSDs include corneal clouding, as with

MPSs I, III, IV, VI, and VII [31,32], or photophobia, as in the case of cystinosis [33,34]. While ERT has significantly improved the life of some LSD patients, only palliative therapy is available for the associated corneal clouding. Some MPS diseases have long been considered potential candidates for gene therapy because of the phenomenon of cross correction and the relatively low level (5–10%) of enzymatic activity needed per cell. The minimum activity needed per cell also translates into the potential to transduce a small fraction of cells that will secrete sufficient quantities of enzyme. This threshold appears to be sufficient to reverse or prevent greater lysosome system (GLS) dysfunction [35], which encompasses recycling, the ubiquitin–proteasome system, all types of autophagy, vesicle biogenesis and turnover, and other pathways.

In this study, we initially assessed the efficacy of CAV-2 vectors for cornea stroma gene transfer in mice, dogs, nonhuman primates and humans. Like HD human Ad vectors [36,37], HD CAV-2 vectors do not contain viral coding regions, which allows a ~30 kb cloning capacity, prolonged transgene expression, and a high safety profile in some tissues [8]. Combining these characteristics with the paucity of cross-reacting pre-existing human immunity [9,10], and the inability to induce dendritic cell maturation [11], makes helper-dependent (HD) CAV-2 vectors powerful tools for clinical gene transfer to post-mitotic cells. An efficient way to transduce stromal keratocytes is to administer vectors via direct intra-stromal injection. This technique causes a transient separation of the stromal matrix allowing the injected bolus to be distributed throughout the corneal stroma. Without this physical separation it is unlikely that any viral vector would be able to diffuse through the stromal matrix. In this way, widespread transduction of the stroma was achieved, in contrast to topical administration following lamellar keratotomy [6,38] or laser ablation [39] of the epithelium, which result in local transduction. Furthermore, as the stroma is delineated by Bowman's and Descemet's membranes, vector dissemination and transduction of the epithelium or endothelium appeared negligible.

Here, CAV-2 vectors were at least as efficient as the HAd5 vectors in all species tested, in particular *in vivo* in nonhuman primates and *ex vivo* in human explants. Previous studies have shown that HAd5 vectors were more efficient than adeno-associated virus (AAV) vectors in mouse corneas over short periods, but integration-defective adenovirus vectors, like those used here, were not as efficient as some AAV serotypes over longer periods [18]. Within 24 h following stromal injection, the cornea of mice and GML returned to the pre-injected transparent state, likely due to the removal of the injected liquid by the pump activity of the endothelial cells. Underlying this transformation is also the efficient and unique repair mechanism intrinsic to the healthy cornea [40], which rapidly restores transparency. However, in MPSs primary accumulation of GAGs and secondary accumulation gangliosides have been linked to numerous complications including chronic inflammation of some tissues. This is relevant when trying to understand the synergy between the chronic inflammation, the mechanical separation of the stroma during injections, and the subsequent activation of the repair mechanism [41]. In 2004, Carlson et al. demonstrated the potential of intrastromal injection by administering a HAd5 vector containing a transgene under control of the keratocan promoter [42]. Consistent with our previous observations, adenovirus-mediated transduction was throughout the mouse cornea,

but peaked after a few days and then declined by 1 week. Although the corneal keratocytes are usually amitotic, they lose their quiescence and differentiate into activated myofibroblasts during repair. Keratocytes immediately adjacent to the lesion begin to undergo apoptosis after injury creating an acellular zone [40], and then neighboring keratocytes become activated, divide, and migrate towards the damaged area. This process is consistent with the loss of the episomal vector genomes. Further studies will be necessary to determine if integrating HD CAV-2 vectors can combine their initial transduction efficiency with long-term expression to exploit the corneal repair mechanism and transduction of precursors that reside in the stroma [43]. These precursors differentiate into keratocytes and restore transparency upon injection into the scarred corneas of mice [43].

To test CAV-2 vector efficacy in a clinically relevant scenario, HD-RIGIE, a helper-dependent CAV-2 vector containing a human GUSB–GFP expression cassette, was tested in the canine MPS VII cornea. Likely due to efficient keratocyte transduction, histological correction of GAG storage and cell morphology was found throughout the MPS VII dog cornea. HD-RIGIE efficacy was due to efficient keratocyte transduction, likely via the use of CAR. CAV-2 vectors appear to have a restricted tropism, compared to HAd5, because they may be “CAR-tropic” and CAV-2 vector efficacy in the keratocytes is likely due to their expression of CAR. Moreover, CAV-1 and CAV-2 have a high degree of similarity in the composition of the capsid proteins, in particular the fiber. In non-vaccinated dogs CAV-1-associated disease is associated with hepatitis and corneal clouding (commonly referred to as blue eye), consistent with the tropism of canine adenoviruses for keratocytes.

Overexpression of GUSB has previously appeared to be well tolerated in most organs and cell types [44]. Based on the relatively low level of β -glu activity found post-HD-RIGIE injection, there is room for increased transcription of the GUSB cassette using a promoter in HD-RIGIE with higher activity in keratocytes. Fusing β -glu to fusing Tat [45] could also increase the therapeutic efficacy. Another combinatorial approach is to eliminate the dominant negative effect of mutant β -glu expression [46] by incorporating an shRNA or microRNAs that would destroy endogenous GUSB mRNAs. This should lead to β -glu tetramers with higher enzymatic activity.

In this study a gradient of β -glu activity was also detected by *in situ* colorimetric assays in the stroma. Keratocytes are sandwiched between the collagen lamellae and responsible for the secretion of the unique stromal extracellular matrix. The collagenous lamellae are made up of heterodimeric complexes of types I/IV collagen fibers arranged in bundles and embedded in a hydrated matrix of glycoproteins and proteoglycans. This stromal meshwork and the avascular nature of the cornea are likely part of the reason that secretion and uptake of β -glu by nontransduced cells was not as efficient as in other tissues [47] and why systemic ERT has little effect on corneal clouding. Alroy et al. [32] characterized MPS I, III, and VI patient corneas and described perturbations that likely influence transparency: the collagen fibrils had an increased mean diameter and altered spacing and irregular packaging. Moreover, the disruption in proteoglycan turnover likely influences collagen fibril size and packaging, which affects transparency. These structural alterations were also similar in MPS I and MPS IV cats. In addition to the disrupted architecture of the collagen fibrils, corneal transparency may be affected by lysosome accumulation [32]. However, the major cause of

corneal opacification appears to be caused by GAG deposits in the stroma, endothelium, and epithelium [48,49].

Due to its comparable size with humans the MPS VII dog cornea is a pertinent model for gene therapy. Compared to laboratory rodents, gene transfer with vectors derived from CAV-2 in dogs presents an interesting setting because in Europe and North America an attenuated replication-competent CAV-2 strain is used as a vaccine to prevent CAV-1 induced hepatitis. Therefore, CAV-2 is ubiquitous in all kennels. One could eventually use this setting (vectors derived from canine pathogens in the canine eye) to evaluate the risks of using human pathogens as vectors for long-term clinical therapy. A challenge concerning the MPS VII dog is understanding and comparing these results to those found in the MPS VII mouse, and what each can teach us about human pathophysiology. For example, mice often poorly mimic many human disease and immunological characteristics, such as inflammation [50]. Yet, there are too few studies in dogs to conclude that they are better indicators of clinical potential. Importantly though, their size and longevity is a key asset.

Acknowledgments

Funding was provided by the European Commission through the European Community's 7th Framework Program (FP7/2007–2013; grant 222992, BrainCAV), the Region Languedoc Roussillon (ARPE and CTP 115277), the Fondation de France (grant # 2008005416), the Vaincre les Maladies Lysosomales (VML 092020), the Agence Nationale de la Recherche (program Blanc: NT09_558711, E-RARE ANR-09-RARE-01 and MNP: ANR-09-MNPS-019-01), NIH grants P40-OD010939, and DK54481, and the Association Française contre les Myopathies. The sponsors had no role in study design; in the collection, analysis and interpretation of data; in the writing of the report; or in the decision to submit the article for publication. We thank the members of EKL for the constructive comments, Nicolas Builles (Montpellier Tissue Bank), staff from Imagerie du Petit Animal de Montpellier, Centre de Ressources en Imagerie Cellulaire de Montpellier, le Réseau d'Histologie Expérimentale de Montpellier, Montpellier RIO Imaging, and IGMM animal house for technical aid and animal care. EJK and VK are Inserm fellows.

References

1. Mehta, A.; Winchester, B. *Lysosomal storage disorders*. Wiley-Blackwell; West Sussex: 2013.
2. Bergwerk KE, Falk RE, Glasgow BJ, Rabinowitz YS. Corneal transplantation in a patient with mucopolysaccharidosis type VII (Sly disease). *Ophthalmic Genet*. 2000; 21:17–20. [PubMed: 10779845]
3. Muenzer J. Overview of the mucopolysaccharidoses. *Rheumatology*. 2011; 50(Suppl 5):v4–v12. [PubMed: 22210669]
4. Neufeld EF. From serendipity to therapy. *Annu Rev Biochem*. 2011; 80:1–15. [PubMed: 21675915]
5. Kremer EJ. Gene transfer to the central nervous system: current state of the art of the viral vectors. *Curr Genomics*. 2005; 6:13–39.
6. Kamata Y, Okuyama T, Kosuga M, O'Hira A, Kanaji A, Sasaki K, Yamada M, Azuma N. Adenovirus-mediated gene therapy for corneal clouding in mice with mucopolysaccharidosis type VII. *Mol Ther*. 2001; 4:307–312. [PubMed: 11592832]
7. Hnasko TS, Perez FA, Scouras AD, Stoll EA, Gale SD, Luquet S, Phillips PE, Kremer EJ, Palmiter RD. Cre recombinase-mediated restoration of nigrostriatal dopamine in dopamine-deficient mice reverses hypophagia and bradykinesia. *Proc Natl Acad Sci U S A*. 2006; 103:8858–8863. [PubMed: 16723393]
8. Soudais C, Skander N, Kremer EJ. Long-term *in vivo* transduction of neurons throughout the rat CNS using novel helper-dependent CAV-2 vectors. *FASEB J*. 2004; 18:391–393. [PubMed: 14688208]
9. Perreau M, Kremer EJ. Frequency, proliferation, and activation of human memory T cells induced by a nonhuman adenovirus. *J Virol*. 2005; 79:14595–14605. [PubMed: 16282459]

10. Perreau M, Guerin MC, Drouet C, Kremer EJ. Interactions between human plasma components and a xenogenic adenovirus vector: reduced immunogenicity during gene transfer. *Mol Ther*. 2007; 15:1998–2007. [PubMed: 17712332]
11. Perreau M, Mennechet F, Serratrice N, Glasgow JN, Curiel DT, Wodrich H, Kremer EJ. Contrasting effects of human, canine, and hybrid adenovirus vectors on the phenotypical and functional maturation of human dendritic cells: implications for clinical efficacy. *J Virol*. 2007; 81:3272–3284. [PubMed: 17229706]
12. Schuchman EH, Toroyan TK, Haskins ME, Desnick RJ. Characterization of the defective beta-glucuronidase activity in canine mucopolysaccharidosis type VII. *Enzyme*. 1989; 42:174–180. [PubMed: 2515056]
13. Kremer EJ, Boutin S, Chillon M, Danos O. Canine adenovirus vectors: an alternative for adenovirus-mediated gene transfer. *J Virol*. 2000; 74:505–512. [PubMed: 10590140]
14. Cubizolle, A.; Serratrice, N.; Skander, N.; Colle, MA.; Ibanes, S.; Gennetier, A.; Bayo-Puxan, N.; Mazouni, K.; Mennechet, F.; Joussemet, B.; Cherel, Y.; Lajat, Y.; Vite, C.; Bernex, F.; Kalatzis, V.; Haskins, ME.; Kremer, EJ. Corrective GUSB transfer to the canine mucopolysaccharidosis VII brain. *Mol Ther*. 2013. <http://dx.doi.org/10.1038/mt.2013.283>
15. Ariza L, Gimenez-Llort L, Cubizolle A, Pages G, Garcia-Lareu B, Serratrice N, Cots D, Thwaite R, Chillon M, Kremer EJ, Bosch A. Central nervous system delivery of helper-dependent canine adenovirus corrects neuropathology and behavior in mucopolysaccharidosis type VII mice. *Hum Gene Ther*. 2014 in press.
16. Soudais C, Boutin S, Kremer EJ. Characterization of cis-acting sequences involved in canine adenovirus packaging. *Mol Ther*. 2001; 3:631–640. [PubMed: 11319926]
17. Sly WS, Quinton BA, McAlister WH, Rimoin DL. Beta glucuronidase deficiency: report of clinical, radiologic, and biochemical features of a new mucopolysaccharidosis. *J Pediatr*. 1973; 82:249–257. [PubMed: 4265197]
18. Hippert C, Ibanes S, Serratrice N, Court F, Malecaze F, Kremer EJ, Kalatzis V. Corneal transduction by intra-stromal injection of AAV vectors *in vivo* in the mouse and *ex vivo* in human explants. *PLoS One*. 2012; 7:e35318. [PubMed: 22523585]
19. Sosnova M, Bradl M, Forrester JV. CD34+ corneal stromal cells are bone marrow-derived and express hemopoietic stem cell markers. *Stem Cells*. 2005; 23:507–515. [PubMed: 15790772]
20. Soudais C, Boutin S, Hong SS, Chillon M, Danos O, Bergelson JM, Boulanger P, Kremer EJ. Canine adenovirus type 2 attachment and internalization: coxsackievirus-adenovirus receptor, alternative receptors, and an RGD-independent pathway. *J Virol*. 2000; 74:10639–10649. [PubMed: 11044108]
21. Bergelson JM, Cunningham JA, Droguett G, Kurt-Jones EA, Krithivas A, Hong JS, Horwitz MS, Crowell RL, Finberg RW. Isolation of a common receptor for Coxsackie B viruses and adenoviruses 2 and 5. *Science*. 1997; 275:1320–1323. [PubMed: 9036860]
22. Tomko R, Xu R, Philipson L. HCAR and MCAR: the human and mouse cellular receptors for subgroup C adenoviruses and group B coxsackieviruses. *Proc Natl Acad Sci*. 1997; 94:3352–3356. [PubMed: 9096397]
23. Zhang Y, Bergelson JM. Adenovirus receptors. *J Virol*. 2005; 79:12125–12131. [PubMed: 16160140]
24. Neufeld EF. Lysosomal storage diseases. *Annu Rev Biochem*. 1991; 60:257–280. [PubMed: 1883197]
25. Sardiello M, Palmieri M, di Ronza A, Medina DL, Valenza M, Gennarino VA, Di Malta C, Donaudy F, Embrione V, Polishchuk RS, Banfi S, Parenti G, Cattaneo E, Ballabio A. A gene network regulating lysosomal biogenesis and function. *Science*. 2009; 325:473–477. [PubMed: 19556463]
26. Mohan RR, Tovey JC, Sharma A, Tandon A. Gene therapy in the cornea: 2005–present. *Prog Retin Eye Res*. 2012; 31:43–64. [PubMed: 21967960]
27. Lai TY, Chan WM, Liu DT, Lam DS. Ranibizumab for retinal angiomatous proliferation in neovascular age-related macular degeneration. *Graefes Arch Clin Exp Ophthalmol*. 2007; 245:1877–1880. [PubMed: 17901972]

28. Yu H, Wu J, Li H, Wang Z, Chen X, Tian Y, Yi M, Ji X, Ma J, Huang Q. Inhibition of corneal neovascularization by recombinant adenovirus-mediated sFlk-1 expression. *Biochem Biophys Res Commun.* 2007; 361:946–952. [PubMed: 17692288]
29. Saika S, Ikeda K, Yamanaka O, Miyamoto T, Ohnishi Y, Sato M, Muragaki Y, Ooshima A, Nakajima Y, Kao WW, Flanders KC, Roberts AB. Expression of Smad7 in mouse eyes accelerates healing of corneal tissue after exposure to alkali. *Am J Pathol.* 2005; 166:1405–1418. [PubMed: 15855641]
30. Galiacy SD, Fournie P, Massoudi D, Ancele E, Quintyn JC, Erraud A, Raymond-Letron I, Rolling F, Maleceze F. Matrix metalloproteinase 14 overexpression reduces corneal scarring. *Gene Ther.* 2011; 18:462–468. [PubMed: 21160532]
31. Williams KA, Coster DJ. Gene therapy for diseases of the cornea — a review. *Clin Experiment Ophthalmol.* 2010; 38:93–103. [PubMed: 19958372]
32. Alroy J, Haskins M, Birk DE. Altered corneal stromal matrix organization is associated with mucopolysaccharidosis I, III and VI. *Exp Eye Res.* 1999; 68:523–530. [PubMed: 10328965]
33. Kalatzis V, Serratrice N, Hippert C, Payet O, Arndt C, Cazeveille C, Maurice T, Hamel C, Maleceze F, Antignac C, Müller A, Kremer EJ. A temporospatial guide to the ocular anomalies in a cystinosis mouse model. *Pediatr Res.* 2007 Aug; 62(2):156–162. [PubMed: 17597652]
34. Nesterova G, Gahl W. Nephropathic cystinosis: late complications of a multisystemic disease. *Pediatr Nephrol.* 2008; 23:863–878. [PubMed: 18008091]
35. Walkley SU. Pathogenic cascades in lysosomal disease — why so complex? *J Inherit Metab Dis.* 2009; 32:181–189. [PubMed: 19130290]
36. Alba R, Bosch A, Chillon M. Gutless adenovirus: last-generation adenovirus for gene therapy. *Gene Ther.* 2005; 12(Suppl 1):S18–S27. [PubMed: 16231052]
37. Amalfitano A, Parks RJ. Separating fact from fiction: assessing the potential of modified adenovirus vectors for use in human gene therapy. *Curr Gene Ther.* 2002; 2:111–133. [PubMed: 12109210]
38. Mohan RR, Hutcheon AE, Choi R, Hong J, Lee J, Ambrosio R Jr, Wilson SE, Zieske JD. Apoptosis, necrosis, proliferation, and myofibroblast generation in the stroma following LASIK and PRK. *Exp Eye Res.* 2003; 76:71–87. [PubMed: 12589777]
39. Bemelmans AP, Arsenijevic Y, Majo F. Efficient lentiviral gene transfer into corneal stroma cells using a femtosecond laser. *Gene Ther.* 2009; 16:933–938. [PubMed: 19387484]
40. Fini ME, Stramer BM. How the cornea heals: cornea-specific repair mechanisms affecting surgical outcomes. *Cornea.* 2005; 24:S2–S11. [PubMed: 16227819]
41. Sindt CW, Lay B, Bouchard H, Kern JR. Rapid image evaluation system for corneal *in vivo* confocal microscopy. *Cornea.* 2013; 32:460–465. [PubMed: 23146928]
42. Carlson EC, Liu CY, Yang X, Gregory M, Ksander B, Drazba J, Perez VL. *In vivo* gene delivery and visualization of corneal stromal cells using an adenoviral vector and keratocyte-specific promoter. *Invest Ophthalmol Vis Sci.* 2004; 45:2194–2200. [PubMed: 15223795]
43. Du Y, Funderburgh ML, Mann MM, SundarRaj N, Funderburgh JL. Multipotent stem cells in human corneal stroma. *Stem Cells.* 2005; 23:1266–1275. [PubMed: 16051989]
44. Vogler C, Galvin N, Levy B, Grubb J, Jiang J, Zhou XY, Sly WS. Transgene produces massive overexpression of human beta-glucuronidase in mice, lysosomal storage of enzyme, and strain-dependent tumors. *Proc Natl Acad Sci U S A.* 2003; 100:2669–2673. [PubMed: 12591953]
45. Orii KO, Grubb JH, Vogler C, Levy B, Tan Y, Markova K, Davidson BL, Mao Q, Orii T, Kondo N, Sly WS. Defining the pathway for Tat-mediated delivery of beta-glucuronidase in cultured cells and MPS VII mice. *Mol Ther.* 2005; 12:345–352. [PubMed: 16043103]
46. Tomatsu S, Orii KO, Vogler C, Grubb JH, Snella EM, Gutierrez M, Dieter T, Holden CC, Sukegawa K, Orii T, Kondo N, Sly WS. Production of MPS VII mouse (Gus(tm(hE540A.mE536A)Sly)) doubly tolerant to human and mouse beta-glucuronidase. *Hum Mol Genet.* 2003; 12:961–973. [PubMed: 12700165]
47. Wolfe JH, Sands MS, Harel N, Weil MA, Parente MK, Polesky AC, Reilly JJ, Hasson C, Weimelt S, Haskins ME. Gene transfer of low levels of beta-glucuronidase corrects hepatic lysosomal storage in a large animal model of mucopolysaccharidosis VII. *Mol Ther.* 2000; 2:552–561. [PubMed: 11124056]

48. Ashworth JL, Biswas S, Wraith E, Lloyd IC. Mucopolysaccharidoses and the eye. *Surv Ophthalmol.* 2006; 51:1–17. [PubMed: 16414358]
49. Ashworth JL, Biswas S, Wraith E, Lloyd IC. The ocular features of the mucopolysaccharidoses. *Eye.* 2006; 20:553–563. [PubMed: 15905869]
50. Seok J, Warren HS, Cuenca AG, Mindrinos MN, Baker HV, Xu W, Richards DR, McDonald-Smith GP, Gao H, Hennessy L, Finnerty CC, Lopez CM, Honari S, Moore EE, Minei JP, Cuschieri J, Bankey PE, Johnson JL, Sperry J, Nathens AB, Billiar TR, West MA, Jeschke MG, Klein MB, Gamelli RL, Gibran NS, Brownstein BH, Miller-Graziano C, Calvano SE, Mason PH, Cobb JP, Rahme LG, Lowry SF, Maier RV, Moldawer LL, Herndon DN, Davis RW, Xiao W, Tompkins RG. Genomic responses in mouse models poorly mimic human inflammatory diseases. *Proc Natl Acad Sci U S A.* 2013; 110:3507–3512. [PubMed: 23401516]

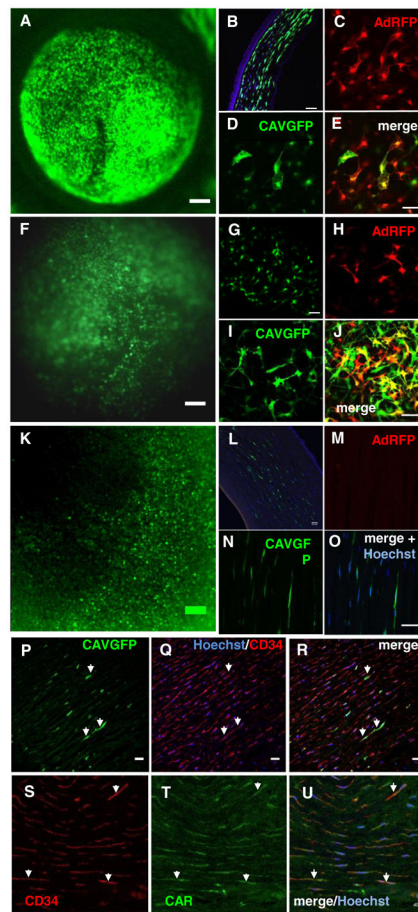


Fig. 1.

Intrastromal injections of CAV-2 and HAd5 vectors *in vivo* in mice, nonhuman primates and *ex vivo* in human cornea. The transduction efficacy of a CAV-2 vector harboring a GFP cassette (CAVGFP) was compared to a HAd5 vector harboring a DsRed II expression cassette (AdRFP) by co-injections. Both expression cassettes were driven by the CMV early promoter to compare efficacy. A tunnel was created across the epithelium at the limbus and was used to introduce a needle. Mice and GML were injected with 1×10^8 pp to 1×10^9 pp of each vector in 20 μ l or 30 μ l of vector, diluted in PBS, respectively. A) *In vivo* imaging of CAVGFP-injected and anesthetized mice using a modified M2BIO stereomicroscope combining a stereo-zoom with macro-objectives and a 20 \times mono-objective. The microscope contained a GFP filters and acquisition was with a CCD (charged-coupled device) camera. The camera was not equipped with a filter to detect DsRed II expression. The small green puncta are GFP positive cells. No GFP signal was detected in the contralateral noninjected eye. Scale bar = 300 μ m. B) Hoechst staining of nuclei and a magnification of 5 \times of a sagittal section allows a global view of GFP expression in the stroma of mice. Scale bar = 50 μ m. C–E) Cornea from injected mice were removed, fixed, and cryosectioned. 10- μ m-thick sagittal sections were screened for DsRed and GFP expression and the images merged to allow a comparison of transduction efficacy. C & D are \sim 1.5-micron-thick confocal planes, while E is a \sim 20-micron-thick confocal stack. Scale bar = 20 μ m. F) GML were injected with 1×10^8 pp of each vector in 30 μ l of vector, diluted in PBS. *In vivo* imaging of CAVGFP- and

AdRFP-injected and anesthetized GML using a stereomicroscope. The small green puncta are GFP positive cells. No GFP signal was detected in the contralateral noninjected eye. Scale bar = 150 μm .G) Hoechst staining of nuclei and a magnification of 5 \times of a sagittal section allows a global view of GFP expression in the stroma of GML. Scale bar = 50 μm .H–J) Corneas from injected GML were removed, fixed, and cryosectioned. 10- μm -thick sagittal sections were screened for DsRed and GFP expression and the images merged to allow a comparison of transduction efficacy. *In vivo* imaging of CAVGFP-injected and anesthetized GML using the M2BIO stereomicroscope. The small green puncta are GFP positive cells. No GFP signal was detected in the contralateral noninjected eye. H & I are ~1.5-micron-thick confocal planes, while J is a ~20-micron-thick confocal stack. Scale bar = 20 μm .K) To determine the efficacy of CAVGFP transduction in human cornea we injected 5×10^9 pp of CAVGFP diluted in 200 μl of PBS. Scale bar = 250 μm .L) 10 \times original magnification of human cornea injected with CAVGFP and AdRFP allows a global view of GFP expression. Scale bar = 50 μm .M–O) Human corneas injected with CAVGFP and AdRFP were fixed, cryosectioned, and 40- μm -thick sagittal sections were screened for GFP and DsRed expression. Scale bar = 40 μm .P–R) Sections from CAVGFP-injected cornea were then incubated with an anti-CD34 antibody, to identify keratocytes, and a secondary antibody labeled with Cy5. The images were merged to demonstrate the preferential transduction of keratocytes (arrows). Scale bar = 20 μm .S–U) Anti-CD34 (in red) and anti-CAR (in green) staining of sagittal sections of human corneas. The merge shows the overlap of CAR and CD34 staining (arrows). Isotypic controls for CAR and CD34 staining can be found in Supplemental Fig. S1.

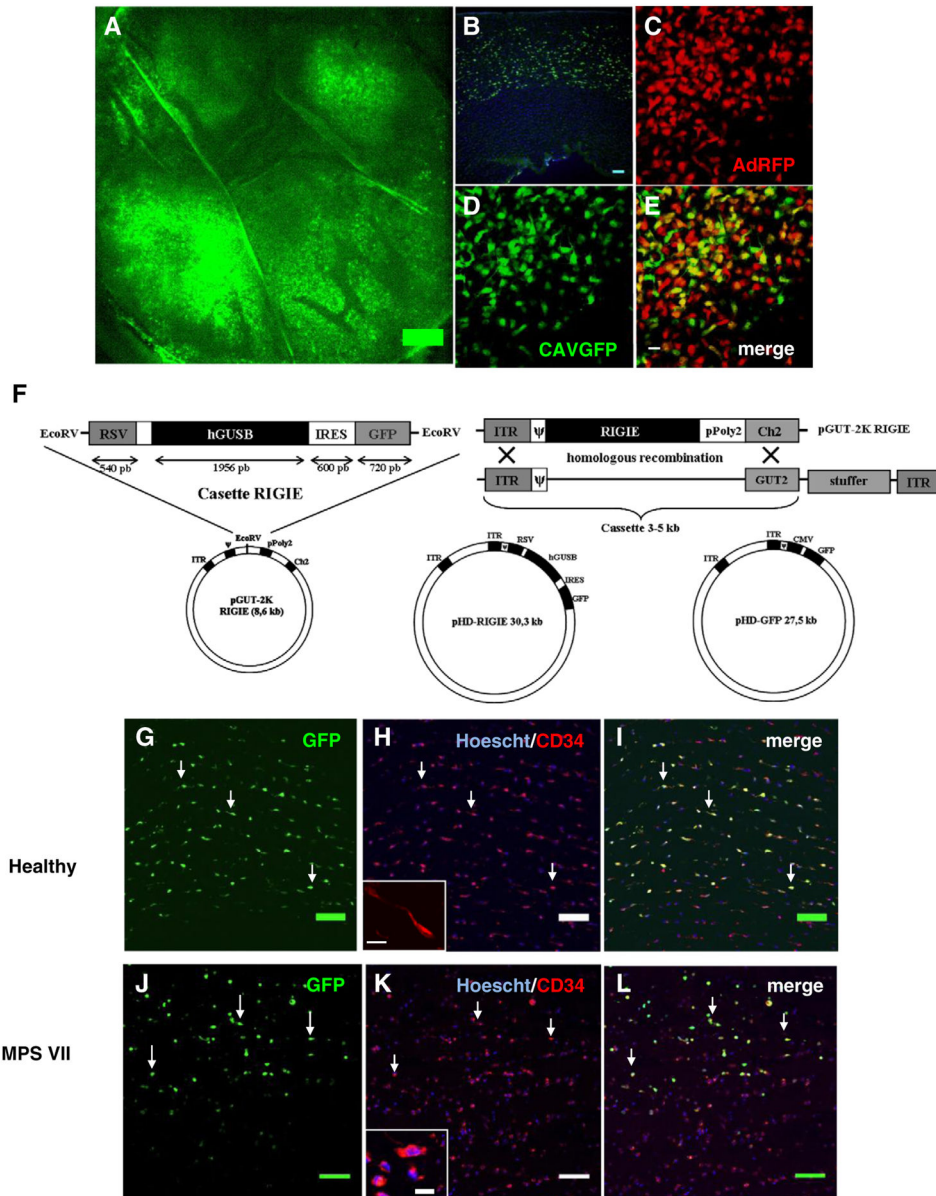


Fig. 2. Intrastromal injections of CAV-2 and HAd5 vectors *ex vivo* in healthy and MPS VII canine cornea. The transduction efficacy of a CAVGFP was compared to a AdRFP in canine cornea by co-injection. A tunnel across the epithelium at the limbus was used to introduce a 33G Hamilton needle and 1×10^9 pp of each vector in 50 μ l of vector, diluted in PBS was injected. **A)** Cornea from healthy dogs injected with CAVGFP and AdRFP. Imaging of CAVGFP-injected using the modified M2BIO stereomicroscope. The small green puncta are GFP positive cells. Scale bar = 500 μ m. **B)** Sagittal section of the canine cornea showing preferential expression of GFP in the stromal cells. Scale bar = 100 μ m. **C–E)** GFP and DsRed expression from the respective vectors and the merge of the two images. Scale bar = 20 μ m. **F)** Schema showing HD-RIGIE cloning approach and GUSB expression cassette.

HD-GFP is a HD CAV-2 vector that contains a CMV early promoter and GFP expression cassette [8]. HD-RIGIE contains the Rous sarcoma virus (RSV) promoter, an artificial intron, the human GUSB cDNA, an internal ribosome entry site, GFP gene and a polyA signal. Cloning, production purification and titration were as previously described [8]. G-I) CAV-2 vector tropism in the healthy canine stroma. Following CAVGFP injections canine cornea were sectioned and stained with anti-CD34 antibodies to determine if the transduced cells were keratocytes. Merge showing overlap of GFP and CD34 signals. Scale bar = 200 μm , and insert = 20 μm .

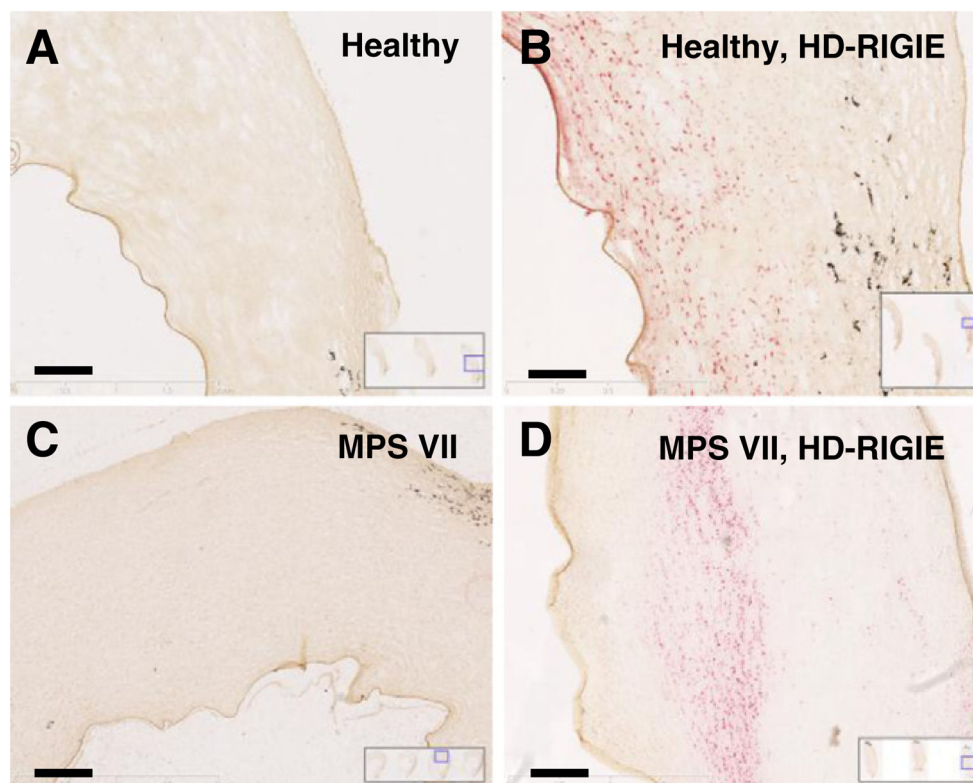


Fig. 3. *In situ* β -glu activity following HD-RIGIE injections in the stroma of the canine MPS VII cornea. Mock-injected or HD-RIGIE-injected MPS VII corneas were analyzed for β -glu activity, as detected by the red precipitate, by an *in situ* colorimetric staining. Corneas were fixed, sectioned and incubated overnight with naphthol-AS-BI- β -D-glucuronide. A) Endogenous β -glu activity in the cornea of healthy dogs is essentially undetectable. Scale bar = 500 μ m. B) HD-RIGIE-mediated β -glu activity in the cornea of healthy dogs, Scale bar = 250 μ m. C) Endogenous β -glu activity cornea of canine MPS VII dogs: Scale bar = 500 μ m. D) HD-RIGIE-mediated β -glu activity in the cornea of canine MPS VII dogs. Scale bar = 250 μ m. NB: Inserts show entire sections on the glass slides.

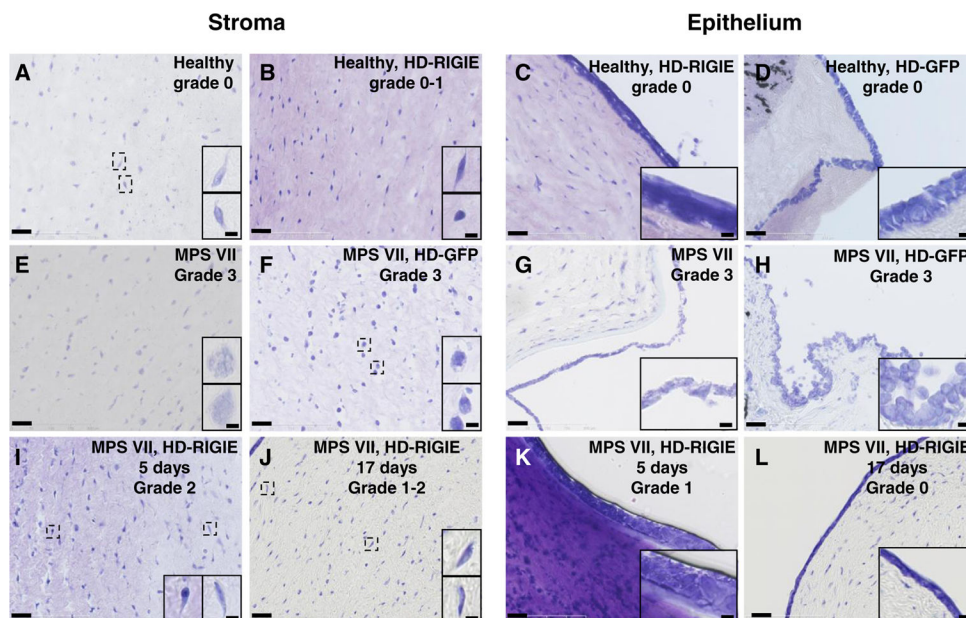


Fig. 4. GAG storage as detected by toluidine blue staining was used to assess MPS VII-related pathology. Mock-injected or HD-RIGIE-injected MPS VII corneas were analyzed for GAG storage as detected by the large nonstaining vacuoles. Corneas were fixed, sectioned and incubated with using toluidine blue. The two columns on the left show the staining in the stroma. The two columns on the right show staining in the epithelium. A–D) Mock-, HD-GFP-, or HD-RIGIE-injected healthy corneas. E–H) Mock- or HD-GFP-injected MPS VII corneas. I–L) HD-RIGIE-injected MPS VII cornea 5 or 17 days post-injection. A masked observer graded the histological anomalies: 0 = no pathology, and 3 = severe pathology. Scale bars: 50 µm and 5 µm in inserts.

imaged, results are expressed \pm S.E.M.). ** p-value < 0.01, *** p-value < 0.001, and **** p-value < 0.0001: Student's t-test.

Author Manuscript

Author Manuscript

Author Manuscript

Author Manuscript

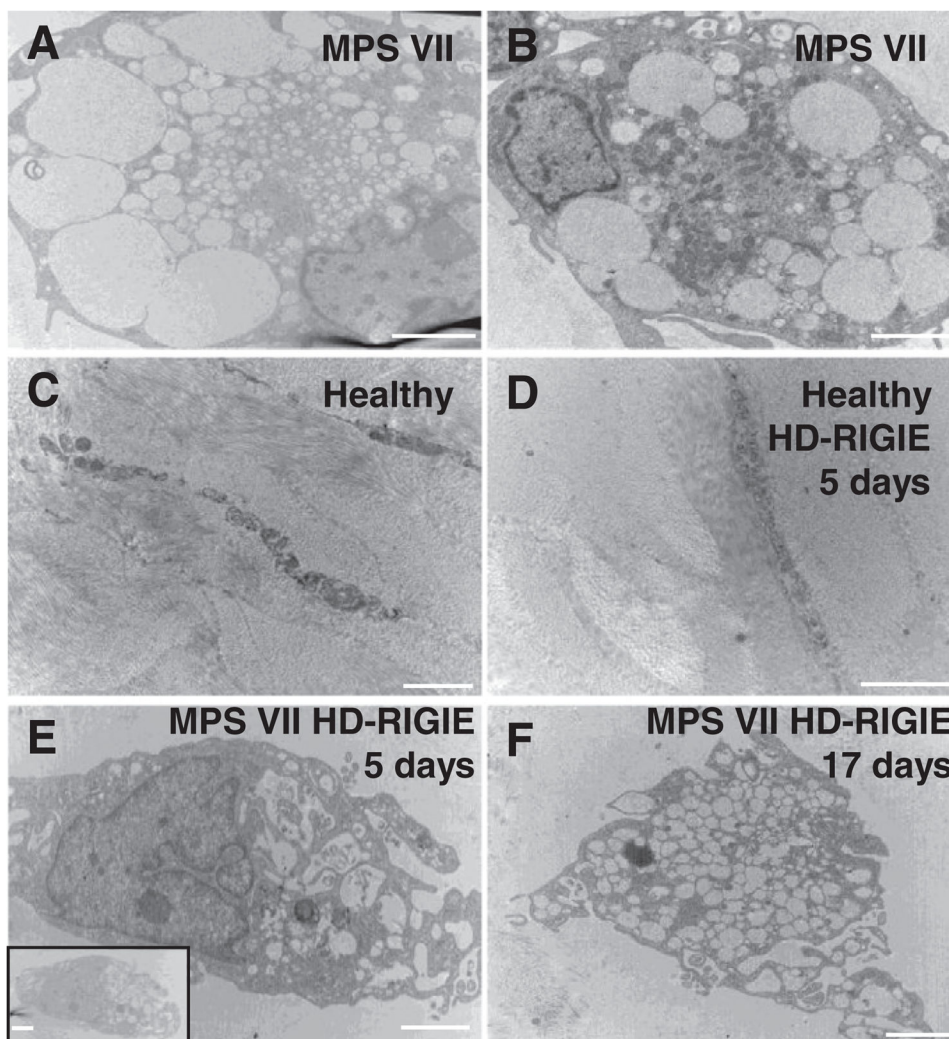


Fig. 6. Transmission electron microscopy (TEM) to analyze HD-RIGIE treated MPS VII cornea. Corneas were prepared for TEM analyses, embedded, sectioned (70-nm thick), counterstained and observed using a Hitachi 7100 TEM. A & B) Mock-treated MPS VII corneas showing enlarged vacuoles. C & D) Healthy dog cornea mock-treated or injected with HD-RIGIE, respectively. E & F) MPS VII dog cornea injected with HD-RIGIE and fixed 5 or 17 days post-injections. Scale bars = 1 μm.

Table 1 β -Glu activity in nmol 4-MU/mg protein/h.

| Noninjected | PBS | HD-GFP | HD-RIGIE |
|----------------|----------------|----------------|---------------|
| Healthy | | | |
| 4.0 \pm 0.2 | 1.9 \pm 0.01 | 3.2 \pm 0.07 | 54 \pm 0.65 |
| MPS VII | | | |
| 1.1 \pm 0.01 | 1.3 \pm 0.07 | 2.4 \pm 0.07 | 15 \pm 0.28 |

Author Manuscript

Author Manuscript

Author Manuscript

Author Manuscript

Table 2

Vesicular storage.

| Cornea | Vesicular storage | |
|------------------------|-------------------|--------|
| | Epithelia | Stroma |
| MPS VII, noninjected | 3 | 3 |
| MPS VII, PBS | 2 | 2 |
| MPS VII, HD-GFP | 2 | 2 |
| MPS VII, 5 d HD-RIGIE | 1 | 2 |
| MPS VII, 17 d HD-RIGIE | 0-1 | 1-2 |
| Healthy, noninjected | 0 | 0 |
| Healthy, HD-GFP | 0 | 0 |
| Healthy, HD-RIGIE | 0 | 0 |

Shading corresponds to the level of vesicular storage, with darker shades representing greater GAG accumulation and lighter shaded little or no GAG storage.